Polyhedron 253 (2024) 116905

Contents lists available at ScienceDirect

Polyhedron

journal homepage: www.elsevier.com/locate/poly

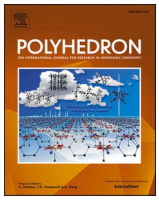

Synthesis and reactivity of a P–H functionalized benzazaphosphole

Miranda P. Howard [a], Preston M. Miura-Akagi [a], Timothy W. Chapp [b], Yuri J.H. Ah-Tye [a], Tomoko Kitano [a], Daniel Y. Zhou [a], Landon G. Balkwill [a], Wesley Y. Yoshida [a], Amy L. Fuller [a], Glenn P.A. Yap [f], Arnold L. Rheingold [c], Gabriela L. Borosky [d,*], Kenneth K. Laali [e,*], Matthew F. Cain [a,*]

[a] Department of Chemistry, University of Hawai'i at Mānoa, 2545 McCarthy Mall, Honolulu, HI 96822, United States
[b] Department of Chemistry, Allegheny College, 520 N. Main Street, Meadville, PA 16335, United States
[c] Department of Chemistry, University of California, 9500 Gilman Drive, La Jolla, San Diego, CA 92093, United States
[d] INFIQC, CONICET and Departamento de Química Teórica y Computacional, Facultad de Ciencias Químicas, Universidad Nacional de Córdoba, Ciudad Universitaria, Córdoba, 5000 Argentina
[e] Department of Chemistry, University of North Florida, 1, UNF Drive, Jacksonville, FL 32224, United States
[f] Department of Chemistry and Biochemistry, University of Delaware, Newark, DE 19716, United States

ARTICLE INFO

Keywords:
Phosphorus
Hydride
Difluorocarbene
Insertion
DFT Calculations

ABSTRACT

Compound **1** was prepared from *N*-Dipp (Dipp = 2,6-diisopropylphenyl) substituted, 10π-electron benzazaphosphole **2** via a two-step protonolysis/substitution protocol using HCl and $LiAlH_4$. As opposed to structurally related *N*-heterocyclic phosphines, the P–H unit in **1** acted as a weak hydride. A sluggish insertion reaction between **1** and electron-poor $CF_3C(O)Ph$ was observed, but dehydrocouplings with weakly acidic alcohols like MeOH and HFIP (hexafluoroisopropanol) did not proceed, as predicted by DFT computations showing high activation energies. However, a rapid and essentially barrierless reaction with $:CF_2$ occurred, yielding P–CF_2H derivative **6**, which was fully characterized by NMR spectroscopy, elemental analysis (EA), HRMS, and X-ray crystallography. The complex splitting pattern of the diastereotopic fluorines of the –CF_2H group observed in the ^{19}F NMR spectrum was successfully simulated using MestReNova. Finally, **1** underwent hydrophosphination in the presence of phenylacetylene, generating a mixture of anti- (***E/Z*-7**) and Markovnikov products (**8**). Computations indicated that anti-Markovnikov ***E*-7** (P–CH=CHPh) formed via highly strained phosphirene intermediate **9**, while ***Z*-7** crystallized out of solution and was characterized by NMR spectroscopy, EA, HRMS, and X-ray crystallography.

1. Introduction

Secondary phosphines of the type R_2P–H (R = alkyl or aryl) are commonly deprotonated with alkyl lithium reagents, generating lithium phosphides ($LiPR_2$) that act as strong nucleophiles (Scheme 1) [1]. Quenching of these nucleophiles with electrophiles represents a fundamental approach to forming new P–C and P–E bonds (E = other element).[2].

However, if the P–H functionality is incorporated into a five-membered ring with flanking amino groups, negative hyperconjugation between the nitrogen lone pairs (N_{LP}) and the σ* orbital of the exocyclic bond triggers an umpolung in reactivity, resulting in a P–H bond that acts as a hydride.[3] When the *N*-substituents are bulky, electron-rich alkyls (R′ = *t*-Bu) and the carbon backbone is unsaturated, these NHPs (**A**, [4] *N*-Heterocyclic Phosphines or DAPs, diazaphospholenes) promote catalytic hydroboration of carbonyls and imines via the two-step insertion/σ-bond metathesis mechanism shown in Scheme 2. [5].

From a bird's eye view, a narrow focus on the five-membered P-containing ring with an adjacent sp^2-hybridized nitrogen group, may lead to the expectation that P–H functionalized benzazaphospholes of Type **B** would behave similarly (Scheme 3, left) [6]. Without the second nitrogen donor though, the delocalization of electron density via $N_{LP} \rightarrow \sigma^*(P–X)$ negative hyperconjugation is essentially cut in half, [7] a finding that was verified by DFT calculations when comparing P-halogenated benzazaphospholes with their NHP counterparts.[8] In that

* Corresponding authors.
E-mail addresses: gborosky@fcq.unc.edu.ar (G.L. Borosky), kenneth.laali@unf.edu (K.K. Laali), mfcain@hawaii.edu (M.F. Cain).

https://doi.org/10.1016/j.poly.2024.116905
Received 10 October 2023; Accepted 17 February 2024
Available online 22 February 2024

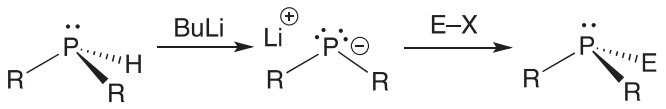

Scheme 1. Deprotonation of secondary phosphines followed by quenching with electrophiles.

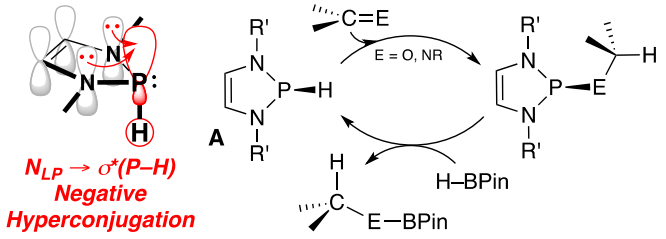

Scheme 2. Negative hyperconjugation in NHPs of Type **A** and catalytic hydroboration of carbonyls and imines.

case, the exocyclic P–X σ* NBO occupancies in NHPs were double that of the analogous benzazaphospholes, consistent with the dramatic elongation of P–X bonds in NHPs that were observed in the solid state.[9] An extension of this phenomenon would suggest that Type **B** derivatives would then have shorter P–H bonds that were less hydridic than **A**. Further compounding this difference, the potent hydridicity displayed by NHPs has been linked to the large contribution of its ionic resonance structure featuring an aromatic 6π-electron phosphenium cation;[10] in fact, the same five-membered C_2N_2P ring with a C–C single bond was calculated to be 100x less nucleophilic than **A**.[11] By comparison, the ionic structure of **B** is not aromatic (sp^3 hybridized benzylic carbon atom) so we expected that P–H functionalized benzazaphospholes of Type **B** would be even weaker hydrides (Scheme 3, right). Here, we report the synthesis of *N*-Dipp substituted **1** and exploratory reactions aimed at gauging its hydridicity, both experimentally and computationally.

2. Results and discussion

2.1. Synthesis of *1*

Exposure of *N*-Dipp substituted, 10π-electron benzazaphosphole **2** to HCl generated chlorophosphine **3**, [7] which when treated with $LiAlH_4$ formed **1**. The two-step sequence could be conducted in a single pot, bypassing the isolation of **3**, or in a stepwise fashion where the chlorophosphine was first isolated by recrystallization before substitution by the hydride; the latter method gave consistently higher yields (Scheme 4).

The identity of **1** was readily confirmed by NMR spectroscopy. A singlet at 25 ppm was observed by $^{31}P\{^1H\}$ NMR spectroscopy (Fig. 1, top left), splitting into a doublet (J_{PH} = 150 Hz) in the ^1H–^{31}P coupled spectrum (top right). The P–H unit resonated as a doublet of doublets of doublets at 6.54 ppm (J_{PH} = 150 Hz, J_{HH} = 4.8 Hz, J_{HH} = 8.4 Hz) in the ^1H NMR spectrum (bottom left) with the diagnostic diastereotopic CH_2 protons observed at 4.66 and 4.24 ppm (bottom right). ^1H NMR spectroscopy also displayed two methines and four methyl groups, consistent with an orthogonally aligned *N*-Dipp group with restricted rotation and *bona fide* evidence that the five-membered ring in C_s-symmetric **2** was dearomatized and functionalized at P to give a C_1-symmetric product.

Ultimately, $^{13}C\{^1H\}$ NMR spectroscopy, elemental analysis, HRMS, and X-ray crystallography confirmed the bulk purity and structure of **1**. As displayed in Figs. 2, **1** crystallized with two independent molecules in the unit cell in the monoclinic space group $P2_1/n$, which was unambiguously determined from the systematic absences. The P1/P1A and P2/P2A disordered pairs were constrained with equal atomic displacement, enabling the refinement of the occupancies at 90/10 and 92/8, respectively. Operating under the assumption that the two molecules are chemically the same, the geometry of the disordered parts was restrained, permitting the location and assignment of the H-atoms on P and the refinement of the average P–H bond distance to 1.47(2) Å.

2.2. Reactions manifesting hydridic character

With a $^1J_{PH}$ = 150 Hz and a P–H bond length of 1.47(2) Å, **1** closely resembled its NHP counterparts (J_{PH} = 150 Hz and 1.51(4) Å).[3] However, unlike NHPs (**A**), which undergo rapid insertions with aldehydes, benzophenone, and α,β-unsaturated aldehydes at room temperature, [12] compound **1** did not react with those substrates and heating the reaction mixtures resulted in the formation of intractable products

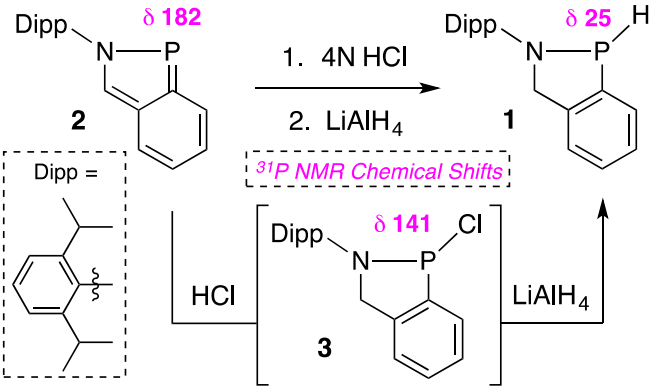

Scheme 4. Synthesis of **1**.

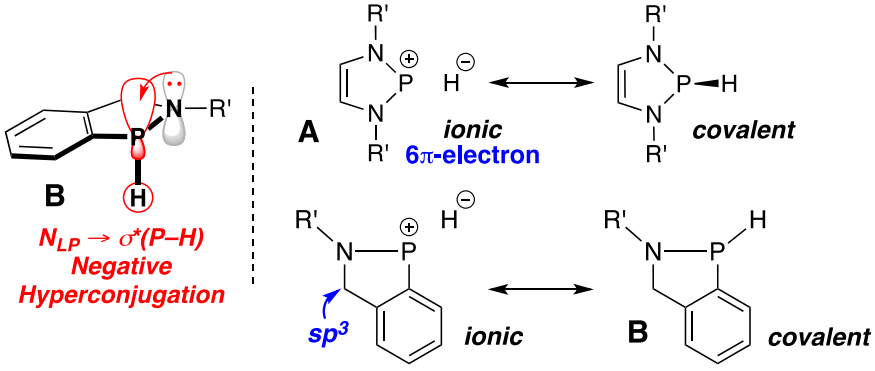

Scheme 3. Negative hyperconjugation in P–H functionalized benzazaphospholes of Type **B** (left) and a comparison of ionic and covalent resonance structures of **A** and **B** (right).

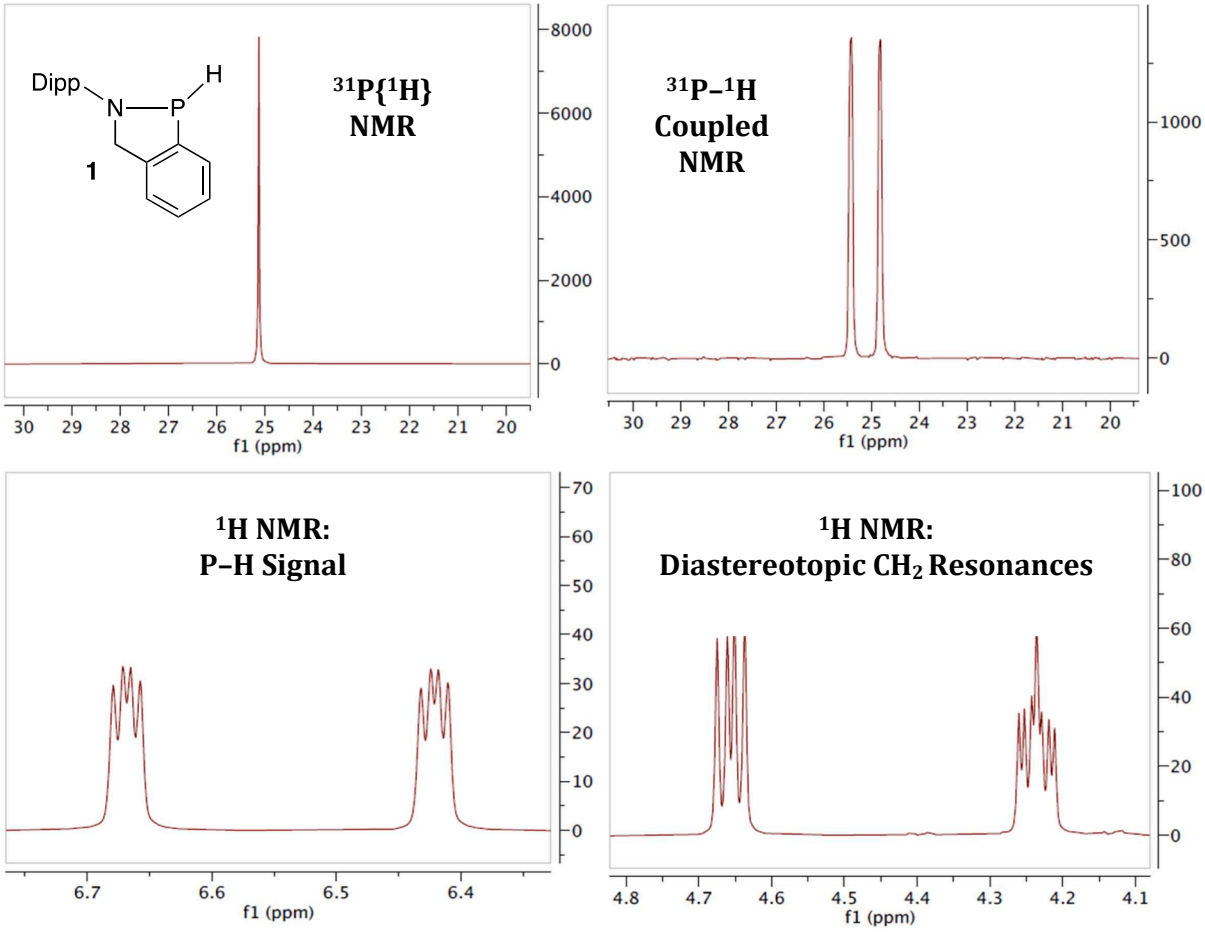

Fig. 1. Selected NMR spectra of **1** in C_7D_8. Top left: $^{31}P\{^{1}H\}$ NMR; Top right: ^{31}P-^{1}H Coupled NMR; Lower left: ^{1}H NMR signal for P–H unit; Lower right: Diastereotopic CH_2 resonances.

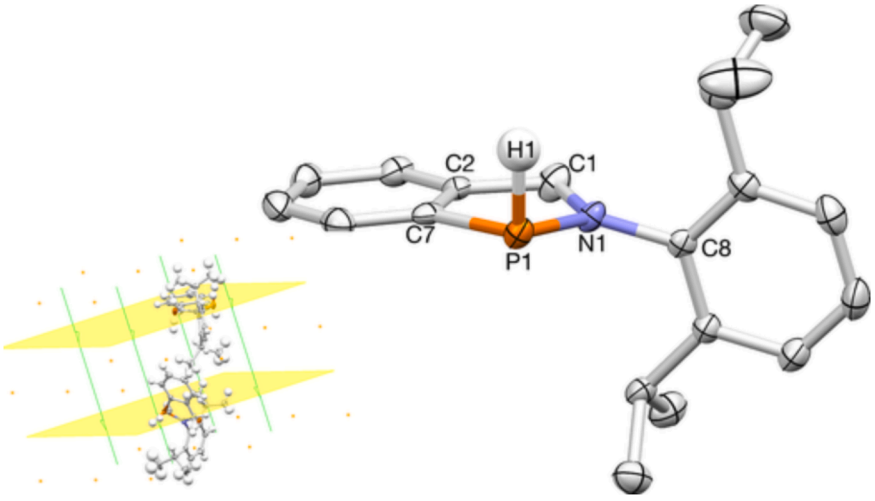

Fig. 2. X-ray crystal structure of one of the two independent molecules of **1**, displaying only the most occupied of the P1/P1A pairing for clarity. Selected bond lengths (Å) and angles (°): P_1–H_1 = 1.47(2), P_1–C_7 = 1.824(2), P_1–N_1 = 1.7222(17), N_1–C_1 = 1.430(3), N_1–P_1–C_7 = 89.06(11), H_1–P_1–C_7 = 100.9(13), N_1–P_1–H_1 = 105.3(13). The unit cell is shown in the inset in the lower left.

(Scheme 5).

On the other hand, use of a more electrophilic ketone like $PhC(O)CF_3$ in toluene at 60 °C gradually consumed **1**, forming diastereomers **4**/**4′** in a 3.6:1 ratio on the basis of $^{31}P\{^{1}H\}$ and ^{19}F NMR spectroscopy (Fig. 3). [13] After 21 h, the insertion reaction reached approximately 75 % conversion, but other unidentified P- and F-containing byproducts were observed. Isolation of the diastereomers from the product mixture at both low and modest conversion could not be accomplished.

Computational modeling (at the B3LYP-D3/6-311+G(d,p) level) of the reaction of **1** with $PhC(O)(CF_3)$ (Fig. 4) showed that insertion of the

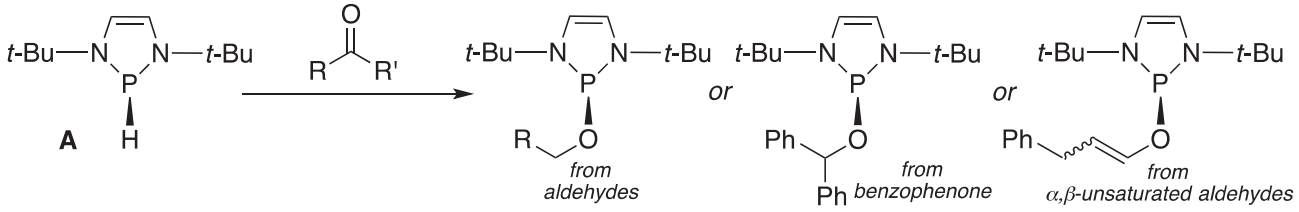

Scheme 5. Insertion reactions of NHPs of Type **A** with carbonyls.

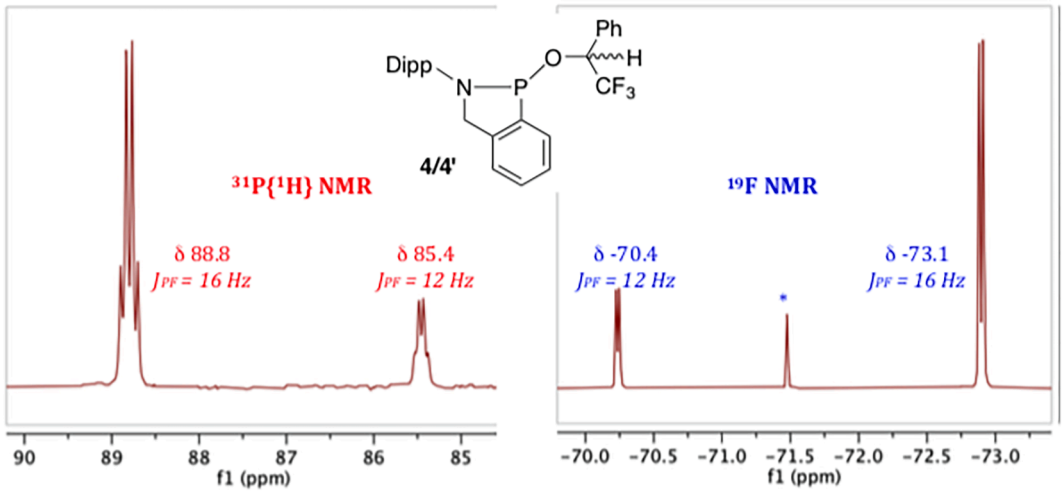

Fig. 3. Selected regions of the $^{31}P\{^{1}H\}$ (left) and ^{19}F NMR (right) spectra (in C_7D_8) highlighting diastereomers **4/4′**. The Asterisk (*) Indicates Remaining $CF_3C(O)Ph$.

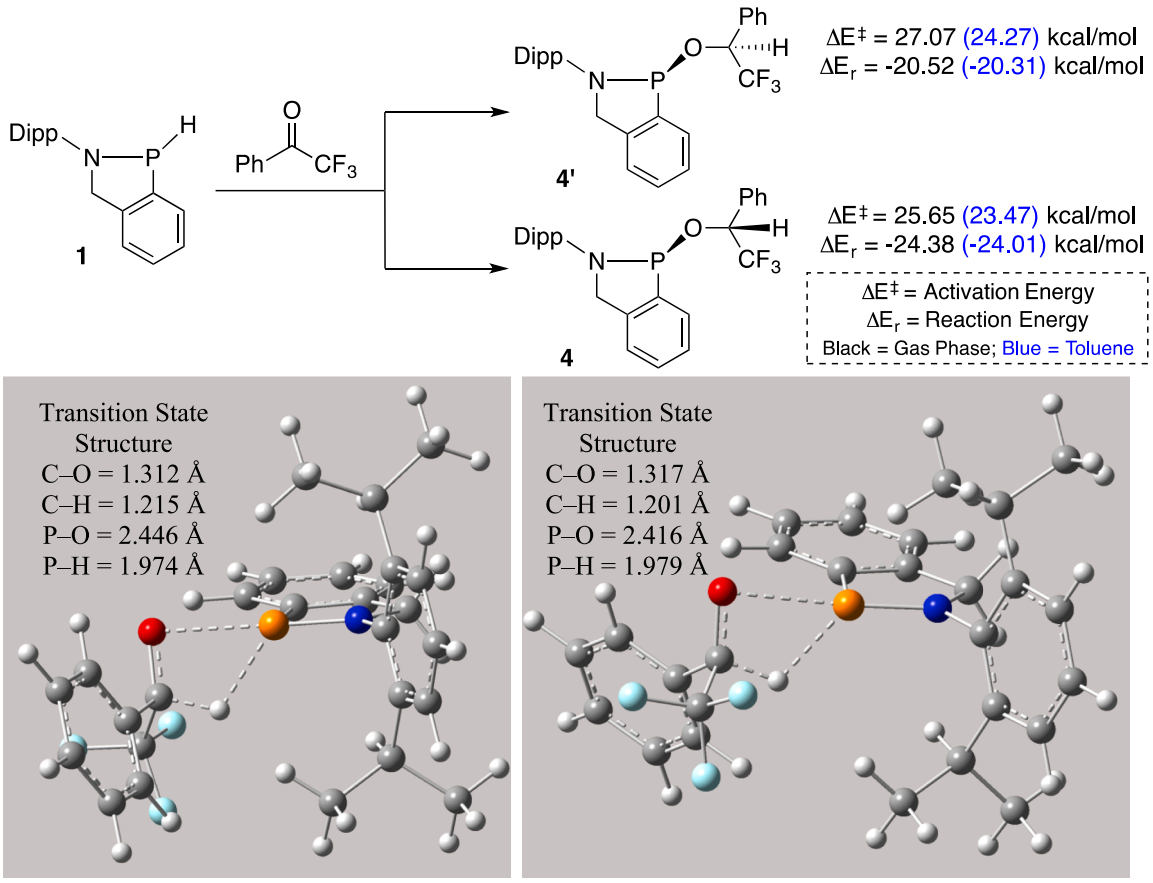

Fig. 4. Computational results for formation of diastereomeric products **4/4′**, showing the structures of the corresponding transition states.

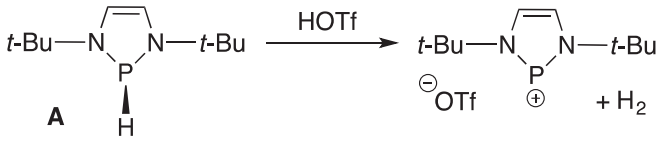

Scheme 6. Protonolysis of NHPs to give phosphenium ions.[15].

P–H bond into the carbonyl proceeded via diastereomeric transition states separated by 0.8 kcal/mol (1.4 kcal/mol in the gas phase), yielding a mixture of diastereomers (**4**/**4′**) that differed in energy by 3.7 kcal/mol (3.9 kcal/mol in the gas phase). Moderate activation energies along with significant exothermicities were calculated for the formation of diastereomers **4**/**4′**, correlating well with the experimental findings.

Another reaction illustrating the hydridic character of NHPs (**A**) was protonolysis,[4] affording phosphenium ions with a weakly coordinating anion (Scheme 6).[14] Analogous protonations on **1** with HOTf or CF_3COOH gave complex product mixtures devoid of any downfield shifted ^{31}P NMR signals (in the 200 ppm range), [15] leading to the suspicion that the resulting phosphenium ion was not stable in solution.

Switching to alcohols like MeOH and HFIP (HFIP, hexafluoroisopropanol, $(CF_3)_2CHOH$) was expected to generate P–OR products (R = Me or $CH(CF_3)_2$) of Type **5** via σ-bond metathesis[16] accompanied by loss of H_2. Experimentally, however, no dehydrocoupling[17] was observed between **1** and either alcohol (Fig. 5). DFT computations revealed that the reaction with MeOH was thermodynamically viable, being exothermic by −1.5 kcal/mol in toluene (−2.0 kcal/mol in the gas phase). However, the transition state was 52.4 kcal/mol higher in energy than the initial complex between the reactants (52.8 kcal/mol in the gas phase). This huge activation energy probably arises from the severe geometric constraints of the four-centered transition state, which involves two highly mobile hydrogen atoms; the related reaction with HFIP had a predicted activation barrier of 45.0 kcal/mol. Both transition states are displayed in Fig. 5. These large computed activation energies justify the absence of reactivity of **1** toward the experimentally tested alcohols.

Therefore, not only does the electronic nature of **1** (one *N*-donor, a non-aromatic ionic phosphenium) lessen its hydridic character, but the reactivity is further attenuated because the fused PN ring system and large *N*-Dipp substituent would create a structural environment not suited to break (O–H and P–H) and form (P–O and H–H) two bonds in

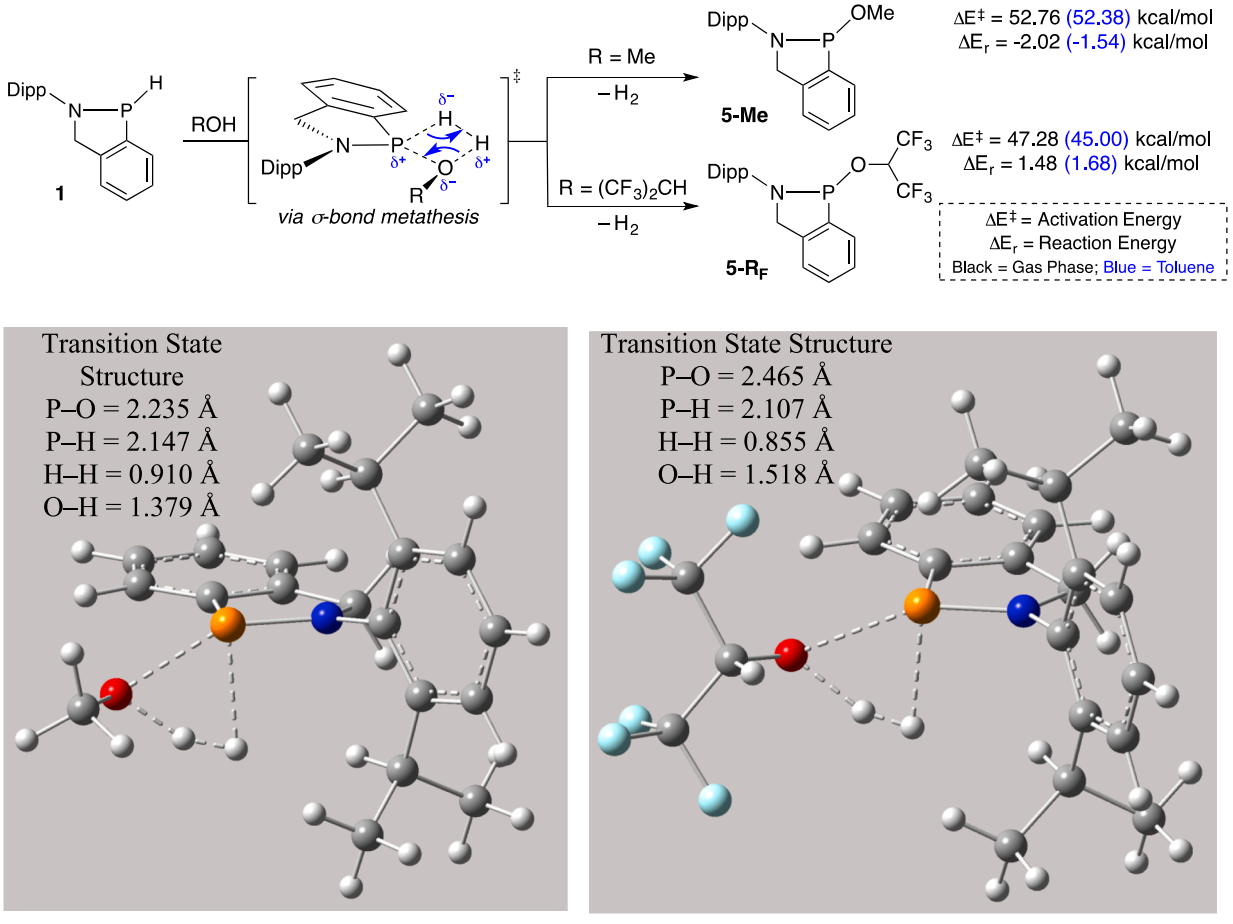

Fig. 5. Computational results for the reactions of **1** with MeOH and HFIP, showing the structures of the corresponding characterized transition states.

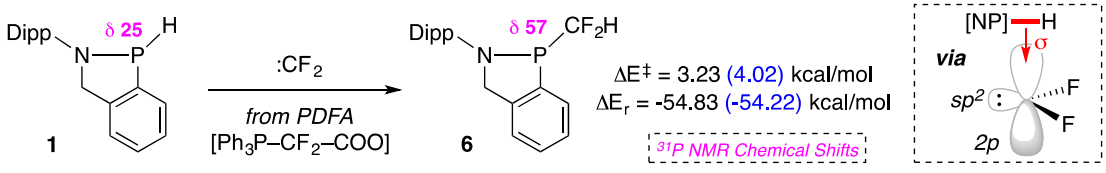

Scheme 7. Synthesis of P–CF_2H analogue **6**.

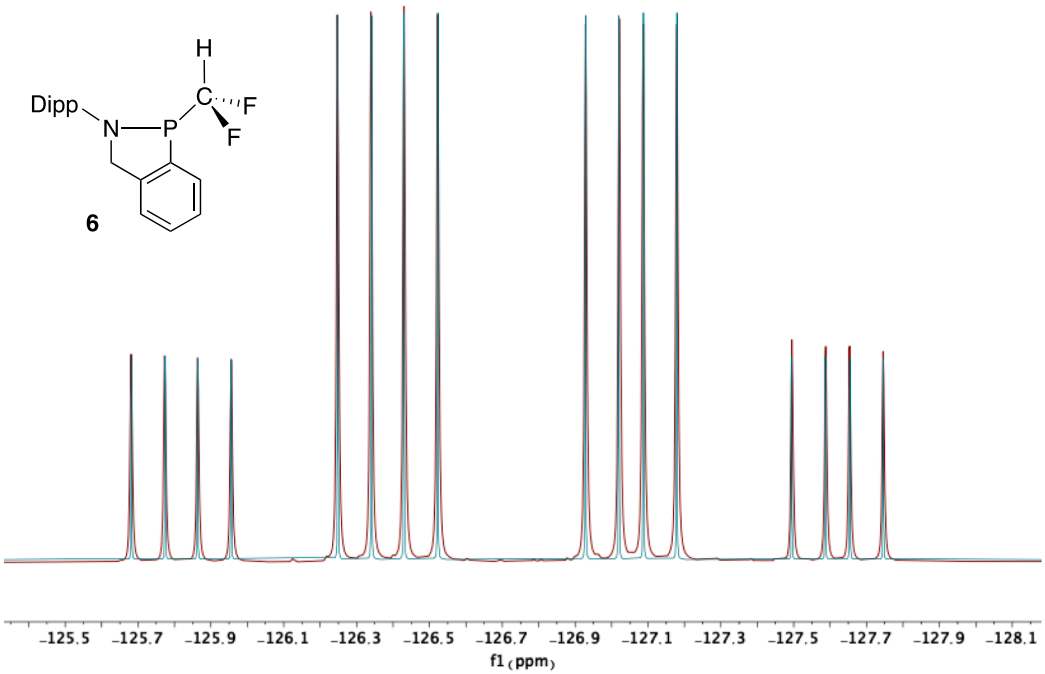

Fig. 6. Experimental (red) and simulated (blue) spectra with ^{19}F NMR (564.10 MHz) signals at −126.182 and −127.279 ppm. (For interpretation of the references to colour in this figure legend, the reader is referred to the web version of this article.)

concert.

2.3. Insertion reactions

Despite its weak hydride donor ability, we speculated that **1** with a polarized (δ+)P–H(δ–) bond might undergo insertions with an electron deficient species. Specifically, a singlet carbene like :CF_2 with an empty *p* orbital seemed poised to accept electron density from the elongated P–H bond in a σ fashion (Scheme 7, right).[18] Indeed, a solution of **1** in toluene reacted with zwitterionic [Ph_3P–CF_2–COO] (PDFA, (triphenylphosphonio)difluoroacetate) in 1 h at 100 °C, affording P–CF_2H analogue **6** and free PPh_3 (and CO_2). Computational modeling of the reaction of **1** with :CF_2 showed an essentially barrierless, highly exothermic reaction, implying that the energy needed to start the reaction in solution is to convert PDFA to :CF_2, [19] which would then undergo instantaneous insertion to give **6**. Treatment of the crude product mixture with xs MeI led to the precipitation of [Ph_3P–Me][I]; a subsequent filtration followed by recrystallization from pentane gave white crystals of **6** (Scheme 7).

The structure of **6** was readily identified by ^{19}F NMR spectroscopy, displaying two distinct doublet of doublets of doublets at −126.1 (J_{FF} = 320 Hz, J_{PF} = 103 Hz, J_{HF} = 52 Hz) and −127.3 (J_{FF} = 320 Hz, J_{PF} = 89 Hz, J_{HF} = 52 Hz) ppm representing the diastereotopic fluorines.[20] The ^{19}F NMR spectrum of **6** is the AB portion of a 2nd order ABMX spin-system that can be simulated using MestReNova (MestReNova 14.3.0 and 14.2.1, more details concerning specific parameters can be found in the Supporting Information) (Fig. 6).

The corresponding $^{31}P\{^1H\}$ NMR spectrum of **6** featured a doublet of doublets at 57 ppm with matching J_{PF} values of 89 and 103 Hz (Fig. 7, top left), and although broadened into an apparent triplet of doublets, a J_{PH} = 18 Hz could be extracted from the ^{31}P–^1H coupled NMR spectrum (top right). The –CF_2H signal resonated as a triplet of doublets at 5.84 ppm (J_{HF} = 52 Hz and J_{PH} = 18 Hz) by ^1H NMR spectroscopy (bottom left), while that same fluorinated carbon also appeared as a triplet of doublets centered at 121.9 ppm (J_{CF} = 272 Hz and J_{CP} = 45 Hz) in the $^{13}C\{^1H\}$ NMR spectrum (bottom right). Overall, the combination of ^1H and $^{13}C\{^1H\}$ NMR spectroscopy confirmed the C_1 symmetric structure as diastereotopic CH_2 protons and two distinct methines and four methyl groups were observed as well.

The structure and bulk purity was further corroborated by X-ray crystallography, HRMS, and elemental analysis (Fig. 8). To the best of our knowledge, **6** represents the first known example of insertion of :CF_2 into a P–H bond of a trivalent P.[21].

Next, questioning if electron-rich substrates may also undergo insertions, **1** was exposed to phenylacetylene in toluene (Scheme 8). Within 1 h at 100 °C, $^{31}P\{^1H\}$ NMR spectroscopy revealed the presence of two major species at 50 and 65 ppm in a ~8:1 ratio, along with a more minor impurity (~5%) at 75 ppm, consistent with a mixture of hydrophosphination products: two anti-(*E*- and *Z*-isomers, **7**) and one Markovnikov-based (**8**).[22].

Recrystallization of this product mixture from hot acetonitrile led to the isolation of X-ray quality crystals of ***Z*-7** (Fig. 9). ^{31}P NMR spectroscopy ($CDCl_3$) confirmed ***Z*-7** corresponded to the signal observed at 50 ppm with a $^3J_{PH}$ = 21 Hz. The ^1H NMR spectrum featured two diagnostic olefinic resonances, both doublets of doublets at 7.02 ($^3J_{PH}$ = 21 Hz) and 6.43 ppm ($^2J_{PH}$ = 4 Hz) with the $^3J_{HH}$ coupling constant (13 Hz), indicative of a *cis*-oriented double bond. $^{13}C\{^1H\}$ NMR spectroscopy combined with HSQC and DEPT experiments definitively identified the presence of these olefinic carbon atoms (δ 140.8 ($^2J_{PC}$ = 19 Hz) and 137.4 ($^1J_{PC}$ = 45 Hz)). Despite the purification process, the most minor impurity (at 75 ppm in the ^{31}P NMR spectrum with $^3J_{PH}$ = 35 Hz) remained stubbornly present in samples of ***Z*-7**. In the ^1H NMR spectrum, two extremely small, but distinct doublets of doublets, corresponding to other olefinic protons were observed at 5.81 and 5.66 ppm with the more upfield of the two signals featuring a $^3J_{PH}$ = 35 Hz and a geminal HH coupling of 2.4 Hz, consistent with the terminal alkene found in Markovnikov product **8**.[23] The remaining product (δ 65) of the crude reaction had no observable J_{PH} coupling in the ^{31}P-^1H coupled NMR spectrum and its olefinic signals were buried / obscured by other signals in the ^1H NMR spectrum, leading to its tentative assignment as ***E*-7**.

From a mechanistic standpoint, the formation of ***E*/*Z*-7** or **8** is fundamentally different than most hydrophosphinations. First and foremost, the P–H bond in **1** is weakly hydridic rather than weakly acidic (like Ph_2P–H), and secondly, the reaction proceeds without any catalyst.[24] We suspected that with a large partial positive charge density (computed as +0.795), the P-center may behave like a metal cation or a

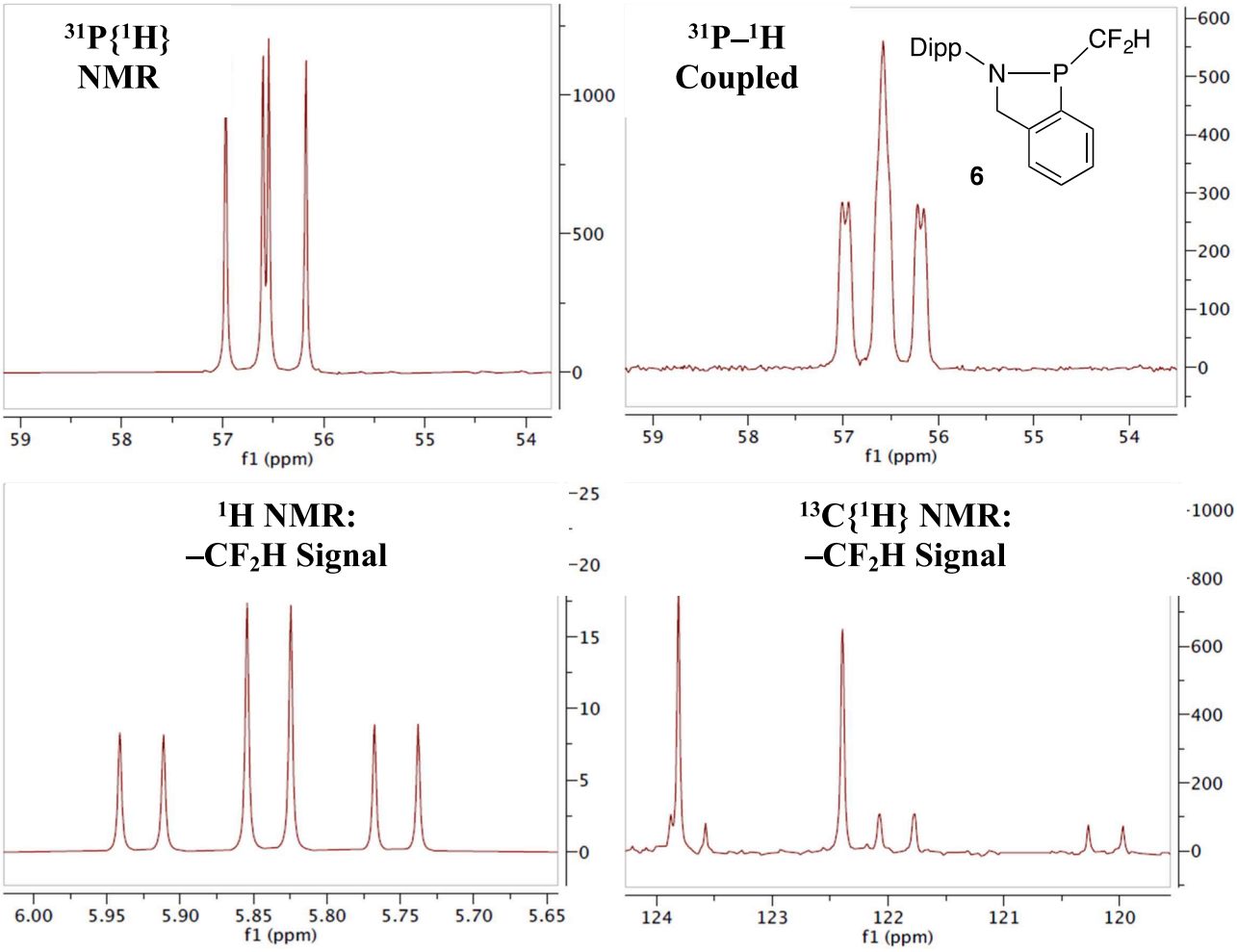

Fig. 7. Selected NMR spectra of P–CF_2H derivative **6** in $CDCl_3$. Top left: $^{31}P\{^1H\}$ NMR; Top right: ^{31}P-^1H Coupled NMR; Lower left: ^1H NMR signal of P–CF_2H proton; Lower right: $^{13}C\{^1H\}$ NMR resonance of P–CF_2H. The two singlets correspond to other Ar signals.

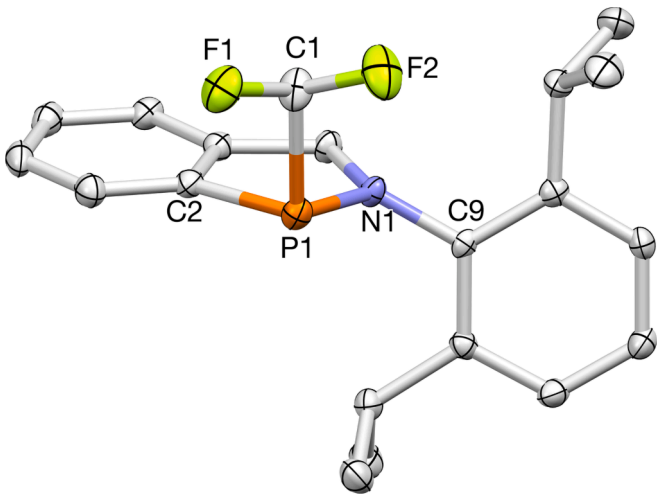

Fig. 8. X-ray crystal structure of **6**. Selected bond lengths (Å) and angles (°): P_1–N_1 = 1.6860(17), P_1–C_2 = 1.823(2), P_1–C_1 = 1.879(2), C_1–F_1 = 1.374(3), C_1–F_2 = 1.370(2), N_1–C_9 = 1.440(2), N_1–P_1–C_2 = 91.22(9), N_1–P_1–C_1 = 101.13 (9), C_2–P_1–C_1 = 92.42(9).

Lewis acid.[25] Computational modeling of the reaction of **1** with phenylacetylene (Fig. 10) revealed that the reaction proceeds via phosphirene[26] intermediate **9** located 19 kcal/mol above the reactants complex (Fig. 11). This species features calculated C–P–C and N–P–C angles of 43.5 and 87.3°, respectively, along with sp^2-hybridized carbons with P–C–C angles of 73.5 and 63.0°, thus being severely strained and predisposed to intramolecular hydride attack. In a second step, concerted ring opening and hydride migration leads to formation of the more thermodynamically stable (by about 4 kcal/mol) trans alkene adduct ***E*-7**. In the second TS, the P–C bond to the internal sp^2-hybridized carbon has already broken, while the hydride migrates from P to C (Fig. 11).

Experimentally though, ***Z*-7** was favored by a ~8:1 ratio as observed by $^{31}P\{^1H\}$ NMR spectroscopy. The intramolecular hydride migration affording the cis alkene analogue would proceed through an open intermediate being about 3 kcal/mol higher in energy than the cyclic phosphirene (Fig. S22); however, the TS corresponding to generation of the cis alkene could not be located. Other catalyst-free hydrophosphinations using phenylacetylene have afforded comparably high *Z* to *E* selectivities (upto 95:5) with the *anti* addition of the P–H bond proposed to occur via a transition state in which two different phosphines, one contributing the PR_2 unit and one donating the H atom, add to opposite faces of the C≡C triple bond.[27] Similarly, formation of ***Z*-7** could result from an intermolecular hydride transfer; however, a more comprehensive computational investigation of the possible mechanistic variations that could generate the *Z*-isomer was out of the scope of the

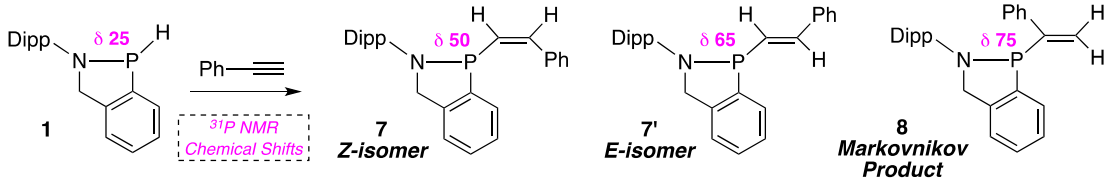

Scheme 8. Products derived from a hydrophosphination reaction between **1** and phenylacetylene.

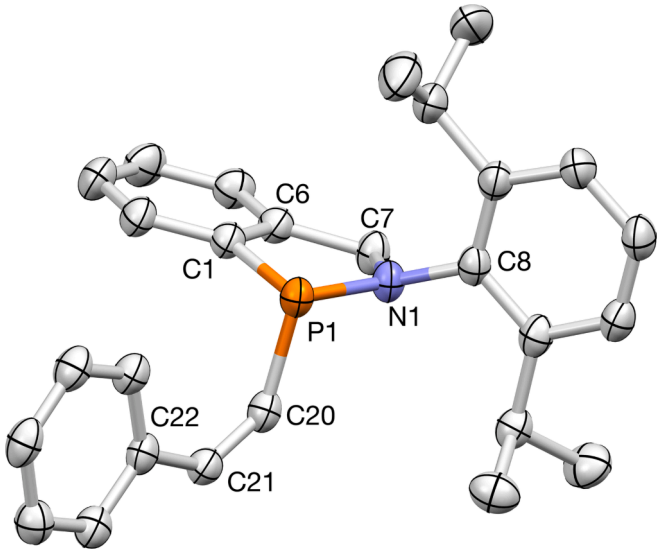

Fig. 9. X-ray crystal structure of ***Z*-7**. Selected bond lengths (Å) and angles (°): P_1–N_1 = 1.7007(18), P_1–C_1 = 1.840(2), P_1–C_{20} = 1.834(2), N_1–C_8 = 1.437(3), N_1–P_1–C_1 = 90.02(9), N_1–P_1–C_{20} = 101.86(10), C_{20}–P_1–C_1 = 96.65(10).

present work.

2.4. Solid state structural comparison

This investigation into the synthesis and preliminary reactivity of **1** yielded X-ray crystal structures of three new benzazaphospholes. The most important solid-state data is compiled in Table 1. Derivatives **1**, **6**, and ***Z*-7** all feature a five-membered C_3NP ring in which the phosphorus is flanked by sp^2-hybridized carbon and nitrogen atoms with a C–P–N angle of roughly 90°. The N–P–X (X = exocyclic group) angle is the most obtuse, but none are more than 106°, reflecting the pyramidal nature of the largely unhybridized, three-coordinate P-center in **1**, **6**, and ***Z*-7**. Like the rest of the structurally characterized benzazaphospholes, **1** is almost perfectly flat at nitrogen (idealized 360°),[7,8] which in combination with more polarizable Lewis Bases or inductively stabilized carbanions as exocyclic groups, is key to maximizing $N_{LP} \rightarrow \sigma^*(P–X)$ negative hyperconjugation. This enhanced delocalization of electron density has previously led to elongated P–I bonds that undergo, as observed by NMR spectroscopy, concentration-dependent bimolecular exchange, [8] and P–CCPh analogues that can facilitate P-to-Pd transmetalation.[7] Here, the planarized nitrogen and soft[28] hydride afforded a lengthened P–H bond (1.47(2) Å) in **1** that, depending on the sterics and electronics of the substrate, engage in reactivity consistent with an ionized structure (like shown in Scheme 3, **B**). On the other hand, P–C derivatives **6** and ***Z*-7** contain the largest deviations from sp^2 at N observed to date (almost 4°). In the case of **6**, this results in a P–R_F bond (R_F = fluorinated alkyl group) that is not elongated relative to its unpublished P–CF_3 counterpart (1.885(2) Å) [29] or other phosphines containing perfluorinated groups.[30] The lack of bond lengthening in ***Z*-7** is even more apparent, as its exocyclic P–C(sp^2) bond is ***shorter*** (1.834(2) Å) than the P–C(sp^2) bond (1.840(2) Å) to the heterocyclic scaffold. Given the P–N bond length of all three derivatives (**1**, **6**, and ***Z*-7**) hovers around 1.7 Å, these structural differences may be rooted in repulsive interactions between the large *N*-Dipp substituent and exocyclic groups that are either sp^3 at carbon (**6**) or sp^2 with a tethered Ph ring (***Z*-7**). The importance of these structural subtleties will become more obvious as we further test the reactivity of **1** and explore the use of **6** and ***Z*-7** as potential transmetalating agents.

2.5. Conclusions

Exposure of *N*-Dipp substituted, 10π-electron benzazaphosphole **2** to HCl generated chlorophosphine **3**, which when treated with $LiAlH_4$ formed **1**. Exploratory reactions between **1** and carbonyls or weakly acidic alcohols demonstrated, and computational modeling supported and/or confirmed, that **1** is a weak hydride. Despite its weak hydridic character, an unprecedented P(III)–H insertion reaction[21] between **1** and :CF_2 was observed, affording P–CF_2H derivative **6**. Furthermore, **1** underwent hydrophosphination in the presence of phenylacetylene to yield anti- (***E*/*Z*-7**) and Markovnikov (**8**) products, perhaps through highly strained phosphirene intermediate **9**.

3. Experimental section

3.1. General experimental details

Unless otherwise specified, all reactions and manipulations were performed under a nitrogen atmosphere in a Vacuum Atmospheres GENESIS glovebox or using standard Schlenk techniques. All glassware was oven-dried overnight (at minimum) at 140 °C prior to use. Anhydrous solvents were purchased directly from chemical suppliers (Aldrich or Acros), pumped directly into the glove box, and stored over oven-activated 4 or 5 Å molecular sieves (Aldrich). 4 N HCl in dioxane, PDFA, phenylacetylene, $CF_3C(O)Ph$, $LiAlH_4$, MeOH, HFIP, and MeI were purchased from chemical suppliers (Aldrich, TCI, Acros). Benzazaphosphole **2** and chlorophosphine **3** were prepared by literature methods.[6,7,8] NMR spectra were obtained on a Varian operating at 300 MHz with frequencies of ^{1}H ($CDCl_3$): 299.841 MHz, ^{13}C: 75.403 MHz, ^{19}F: 282.107 MHz, and ^{31}P: 121.386 MHz or a Bruker 600 MHz spectrometer with frequencies of ^{1}H ($CDCl_3$): 599.567 MHz, ^{13}C: 150.776 MHz, ^{19}F: 564.097 MHz, and ^{31}P: 242.726 MHz. All spectra are displayed in the Supporting Information. NMR chemical shifts are reported as ppm relative to tetramethylsilane and are referenced to the residual proton or ^{13}C signal of the solvent (^{1}H $CDCl_3$, 7.27 ppm; ^{1}H C_6D_6, 7.16 ppm; ^{13}C $CDCl_3$, 77.16 ppm; ^{13}C C_6D_6, 128.06 ppm).

3.2. Synthesis of *1*

In two separate vials, chlorophosphine **3**[7] (994 mg, 3.00 mmol) was dissolved in 10 mL of diethyl ether, while lithium aluminum hydride ($LiAlH_4$) (227 mg, 6.00 mmol, 2 equiv) was suspended in 10 mL of diethyl ether. Both were stored at −35 °C for 30 min, then combined in a 250 mL round bottom flask, and stirred for 30 min. Unreacted $LiAlH_4$ was filtered off through a celite plug on a frit, and the filtrate was pumped down under vacuum and extracted with pentane (3 x 10 mL) then run through a silica plug. The eluent containing the crude product was analyzed by ^{31}P{^{1}H} NMR spectroscopy, confirming the presence of

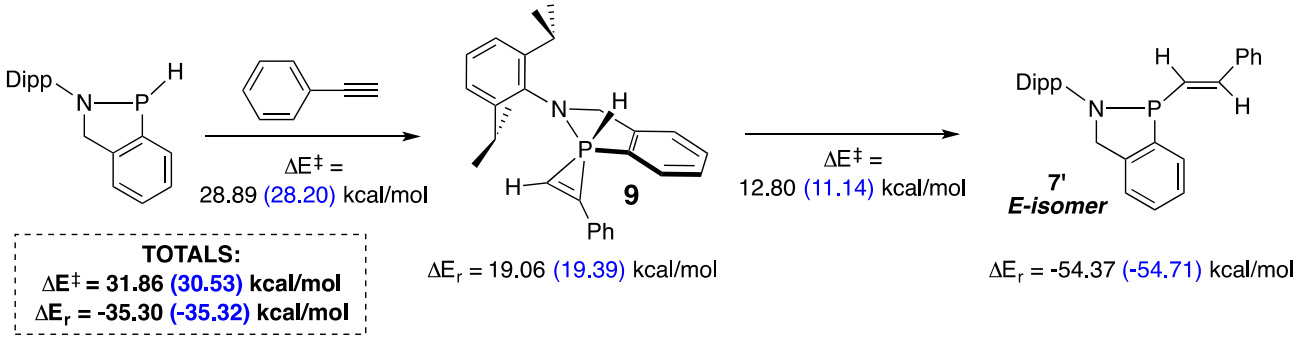

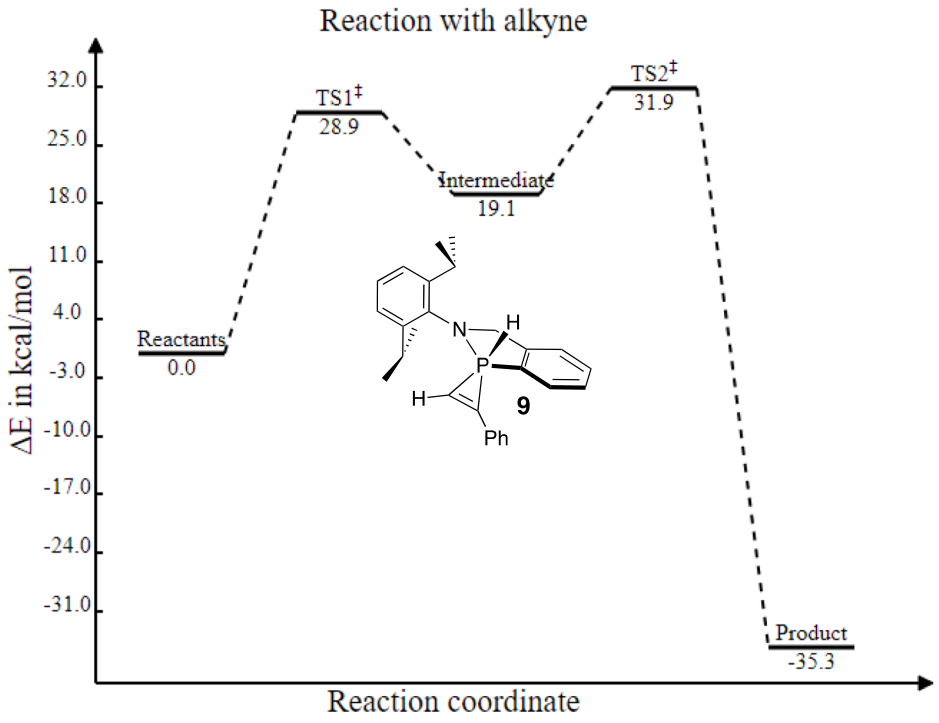

Fig. 10. Computational results for the reaction of 1 with phenylacetylene.

the P–H heterocycle at δ 25 ppm. The fraction was concentrated to 10 mL in pentane and stored at −35 °C, yielding white, X-ray quality crystals of the product (398 mg, 1.34 mmol, 45 %). A second crop of white crystalline solid was isolated by concentrating the mother liquor to 5 mL and storing at −35 °C (52 mg, 0.175 mmol, 6 %). Totals = 450 mg, 1.51 mmol, 51 %. The modest yield (~50 %) of product is not due to complex crude reaction mixtures, but rather originates from extremely high solubility in most commonly employed glovebox solvents. Only highly concentrated solutions in pentane at low temperature for extended periods of time resulted in precipitation.

Anal. Calcd for $C_{19}H_{24}NP$: C, 76.74; H, 8.13; N, 4.71. Found: C, 76.95; H, 8.39; N, 4.62. HRMS *m/z* calcd for $C_{19}H_{24}NPO$ $(M+H)^+$: 314.1668. Found: 314.1672. This is the product of rapid hydrolysis to the P–OH derivative. $^{31}P\{^1H\}$ NMR (243 MHz, C_7D_8): δ 25.1. ^{31}P NMR (243 MHz, C_7D_8): δ 25.1 (d, J_{PH} = 150 Hz). ^1H NMR (600 MHz, C_7D_8): δ 7.35 (br m, 1H, Ar), 7.15 (t, J = 8 Hz, 1H, Ar), 7.05 (br m, 4H, Ar), 6.99 (m, 1H, Ar), 6.54 (ddd, J = 150, 8.4, and 4.8 Hz, 1H, PH), 4.66 (dd, J = 14.4 and 8.4 Hz, 1H, CH_2), 4.24 (ddd, J = 14.4, 10.2 (PH coupling), and 4.8 Hz, 1H, CH_2), 3.33 (septet, J = 7 Hz, 1H, CH), 3.05 (septet, J = 7 Hz, 1H, CH), 1.23 (overlapping d, J = 7 Hz, 6H, 2 CH_3), 1.16 (d, J = 7 Hz, 3H, CH_3), 1.05 (d, J = 7 Hz, 3H, CH_3). $^{13}C\{^1H\}$ NMR (151 MHz, C_7D_8): δ 150.7 (s, Ar), 148.8 (s, Ar), 145.6 (s, Ar), 140.9 (d, J = 15 Hz, Ar), 138.8 (s, Ar), 128.2 (s, CH Ar), 127.7 (s, CH Ar), 127.5 (d, J = 35 Hz, CH Ar), 127.3 (d, J = 18 Hz, CH Ar), 124.5 (s, CH Ar), 123.9 (s, CH Ar), 122.4 (s, CH Ar), 64.4 (d, J = 11 Hz, CH_2), 28.9 (s, CH), 28.7 (s, CH), 25.2 (s, Me), 25.0 (d, J = 3 Hz, Me), 24.2 (s, Me), 24.1 (s, Me). ^1H and ^{13}C NMR assignments were supported by HSQC and DEPT experiments. Note: The aryl signals in $^{13}C\{^1H\}$ NMR spectrum were somewhat obscured by C_7D_8, and **1** is insoluble in C_6D_6 and decomposes in $CDCl_3$ and CD_2Cl_2.

3.3. *Generation of diasteromeric mixture of **4/4'***

Compound **1** (20 mg, 0.067 mmol) was dissolved in 1 mL of toluene and was transferred to an NMR tube fitted with a rubber septum. The tube was taken out of the glove box and $CF_3C(O)Ph$ (10 μL, 0.071 mmol, 1.1 equiv.) was injected via syringe. The clear and homogenous reaction mixture was then analyzed by $^{31}P\{^1H\}$ NMR and ^{19}F NMR spectroscopy. At room temperature, the reaction was extremely sluggish (<5% conversion). However, with heating at 60 °C, conversion to the diastereomeric products was observed. After 21 h at approximately 75 % conversion, the two diastereomers were present at δ 88.8 and 85.4 ppm in a 3.6:1 ratio as determined by $^{31}P\{^1H\}$ NMR spectroscopy. The matching signals and integrations were observed at δ −70.4 and −73.1 ppm in the ^{19}F NMR spectrum. Prolonged heating at 60 °C led to more pronounced side products and little to no additional conversion of **1**.

HRMS *m/z* calcd for $C_{27}H_{30}F_3NOP$ $(M+H)^+$: 472.2012. Found: 472.2010. $^{31}P\{^1H\}$ NMR (243 MHz, C_7H_8): δ 88.8 (quartet, J_{PF} = 16 Hz, major diastereomer), 85.4 (quartet, J_{PF} = 12 Hz, minor diastereomer).

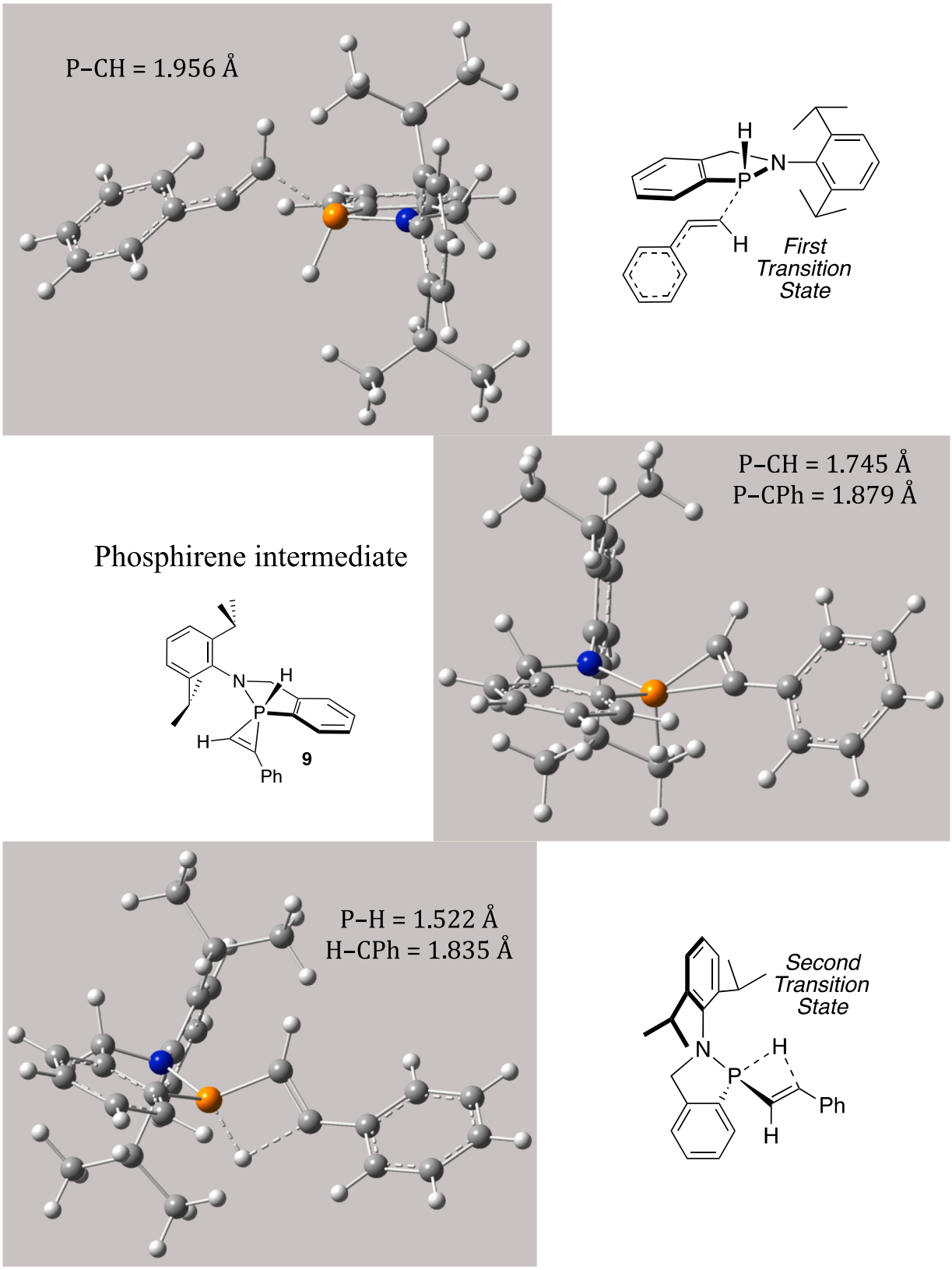

Fig. 11. Reaction of **1** with phenylacetylene: the structures of both transition states and phosphirene intermediate **9** leading to the formation of the ***E*-7**.

^{19}F NMR (564 MHz, C_7H_8): δ −70.4 (doublet, J_{FP} = 12 Hz, minor diastereomer) and −73.1 ppm (doublet, J_{FP} = 16 Hz, major diastereomer). See Supporting Information for ^{1}H and ^{13}C{^{1}H} NMR, COSY, HSQC, and HMBC spectra: some additional assignments are provided.

3.4. Synthesis of P–CF_2H derivative ***6***

Compound **1** (275 mg, 0.925 mmol) and (triphenylphosphino) difluoroacetate (PDFA) (395 mg, 1.11 mmol, 1.2 equiv) were combined

Table 1
Selected X-ray Crystallographic data for **1**, **6**, and ***Z*-7**.

	P–H (1)	P–CF_2H (6)	P–CH=CHPh (*Z*-7)
Σ of angles @ P	295.26°	284.77°	288.53°
P–X bond	1.47(2) Å	1.879(2) Å	1.834(2) Å
P–C bond	1.824(2) Å	1.823(2) Å	1.840(2) Å
P–N bond	1.7222(17) Å	1.6860(17) Å	1.7007(18) Å
Σ of angles @ N	359.76°	356.15°	356.48°

in a vial, dissolved in 10 mL of toluene, and transferred to a Schlenk bomb fitted with a screw-top Teflon cap. The homogeneous solution was heated for 1 h at 100 °C, turning pale yellow. Subsequent analysis by $^{31}P\{^1H\}$ and ^{19}F NMR spectroscopy confirmed complete conversion to product as well as the presence of the PPh_3 byproduct (δ −5.6, singlet, $CDCl_3$). The crude product mixture was returned to the glovebox and iodomethane (580 μL, 9.25 mmol, 10 equiv) was injected to precipitate the phosphonium salt [Ph_3P-Me][I]. After stirring for 30 min, the solid was filtered off, and the filtrate was concentrated under vacuum. The residue was extracted with pentane (3 x 10 mL) and filtered through a silica plug in a pipette. This fraction was concentrated to 20 mL in pentane and stored at −35 °C, yielding white crystals suitable for X-ray diffraction (126 mg, 0.363 mmol, 39 %). A second crop of white crystalline solid was obtained by concentrating the mother liquor to 10 mL and cooling to −35 °C (86 mg, 0.248 mmol, 27 %). Totals = 212 mg, 0.611 mmol, 66 %.

Anal. Calcd for $C_{20}H_{24}F_2NP$: C, 69.15; H, 6.96; N, 4.03. Found: C, 68.93; H, 6.99; N, 3.93. HRMS *m/z* calcd for $C_{20}H_{24}F_2NP$ $(M+H)^+$: 348.1687. Found: 348.1674. $^{31}P\{^1H\}$ NMR (243 MHz, $CDCl_3$): δ 56.6 (dd, $^2J_{PF}$ = 89, 103 Hz). ^{31}P NMR (243 MHz, $CDCl_3$): δ 56.6 ($^2J_{PH}$ = 18 Hz). ^{19}F NMR (564 MHz, $CDCl_3$): δ −126.1 (ddd, $^2J_{FH}$ = 52 Hz, $^2J_{FP}$ = 103 Hz, and $^2J_{FF}$ = 320 Hz, 1F, CF_2H) and −127.3 (ddd, $^2J_{FH}$ = 52 Hz, $^2J_{FP}$ = 89 Hz, and $^2J_{FF}$ = 320 Hz, 1F, CF_2H). ^1H NMR (600 MHz, $CDCl_3$): δ 7.70 (m, 1H, Ar), 7.47 (m, 1H, Ar), 7.44 (m, 1H, Ar), 7.39 (d, J = 8 Hz, 1H, Ar), 7.29 (m, 1H, Ar), 7.18 (overlapping m, 2H, Ar), 5.84 (apparent td, $^2J_{PH}$ = 18 Hz and $^2J_{FH}$ = 52 Hz, 1H, CF_2H), 5.10 (d, $^2J_{HH}$ = 14 Hz, 1H, CH_2), 4.30 (dd, $^2J_{HH}$ = 14 Hz and $^3J_{PH}$ = 8 Hz, 1H, CH_2), 3.57 (septet, J = 7 Hz, 1H, CH), 2.68 (septet, J = 7 Hz, 1H, CH), 1.28 (d, J = 7 Hz, 3H, Me), 1.26 (d, J = 7 Hz, 3H, Me), 1.23 (d, J = 7 Hz, 3H, Me), and 1.06 (d, J = 7 Hz, 3H, Me). $^{13}C\{^1H\}$ NMR (151 MHz, $CDCl_3$): δ 149.8 (s, Ar), 147.5 (s, Ar), 145.7 (s, Ar), 140.4 (d, J = 17 Hz, Ar), 134.9 (apparent t, J = 6 Hz, Ar), 129.6 (s, CH Ar), 129.0 (d, J = 24 Hz, CH Ar), 127.5 (overlapping, 2 CH Ar), 124.6 (s, CH Ar), 123.8 (s, CH Ar), 122.4 (s, CH Ar), 121.9 (td, $^1J_{CP}$ = 45 Hz and $^1J_{CF}$ = 272 Hz, CF_2H), 64.6 (d, J = 9 Hz, CH_2), 28.6 (d, J = 6 Hz, CH), 28.0 (s, CH), 25.3 (s, Me), 25.0 (s, Me), 24.5 (d, J = 4 Hz, Me), 24.0 (s, Me). ^1H and ^{13}C NMR assignments were supported by HSQC and DEPT experiments.

3.5. Synthesis of P–CH=CHPh Analogue *Z*-7

Compound **1** (60 mg, 0.202 mmol) was dissolved in 10 mL of toluene and transferred to a 25 mL Schlenk bomb fitted with a screw-top Teflon cap and a stir bar. Under positive nitrogen pressure, a septum was installed and phenylacetylene (0.066 mL, 0.605 mmol, 3 equiv) was injected via syringe. The bomb was resealed and heated with stirring at 100 °C for 2 h. The reaction was brought back into glovebox and filtered through celite in a pipette fitted with a Kimwipe plug. The filtrate was concentrated under vacuum and analyzed by $^{31}P\{^1H\}$ NMR spectroscopy, confirming the presence of tentatively assigned cis- and trans-isomers in an 8:1 ratio at δ 50 and 65 ppm; a more minor product at δ 75 ppm was also observed. The crude product was suspended in acetonitrile (1 mL) in a 25 mL Schlenk bomb, removed from glovebox, and heated at 80 °C for 15 min until it was homogeneous. After cooling to room temperature, it was further cooled at 0 °C overnight, yielding X-ray quality crystals of the major product (23 mg, 0.058 mmol, 28 %). A second crop was obtained by concentrating the mother liquor under vacuum and repeating the recrystallization process, affording more product (11 mg, 0.028 mmol, 14 %). Totals = 34 mg, 0.085 mmol, 42 %. The mediocre yield of product (<50 %) is not due to the generation of other byproducts (besides the isomers), but rather originates from extremely high solubility in most commonly employed glovebox solvents. In acetonitrile at room temperature, these insertion products are somewhat soluble, but with heating, the mixtures become homogeneous and slow cooling yielded precipitation of crystalline material.

Anal. Calcd. for $C_{27}H_{30}NP$: C, 81.17; H, 7.57; N, 3.51. Found: C, 80.89; H, 7.65; N, 3.36. HRMS *m/z* calcd for $C_{27}H_{30}NP$ $(M+H)^+$: 400.2189. Found: 400.2189. $^{31}P\{^1H\}$ NMR (243 MHz, $CDCl_3$): δ 49.9. ^{31}P NMR (243 MHz, $CDCl_3$): δ 49.9 (d, J_{PH} = 21 Hz). ^1H NMR (600 MHz, $CDCl_3$): 7.61 (br t, J = 6 Hz, 1H, Ar), 7.51 (d, J = 8 Hz, 2H, Ar), 7.39 (m, 3H, Ar), 7.28 (m, 4H, Ar), 7.20 (d, J = 8 Hz, 1H, Ar), 7.15 (d, J = 8 Hz, 1H, Ar), 7.02 (dd, J = 13 Hz and 21 Hz, 1H, olefinic = CHPh), 6.43 (dd, J = 4 Hz and 13 Hz, 1H, olefinic P–CH=), 5.18 (d, J = 14 Hz, 1H, CH_2), 4.40 (dd, J = 9 Hz and 14 Hz, 1H, CH_2), 3.66 (septet, J = 7 Hz, 1H, CH), 2.95 (septet, J = 7 Hz, 1H, CH), 1.31 (d, J = 7 Hz, 3H, CH_3), 1.24 (d, J = 7 Hz, 3H, CH_3), 1.16 (d, J = 7 Hz, 3H, CH_3), 1.12 (d, J = 7 Hz, 3H, CH_3). $^{13}C\{^1H\}$ NMR (151 MHz, $CDCl_3$): δ 149.9 (s, Ar), 148.6 (s, Ar), 143.8 (s, Ar), 143.1 (s, Ar), 141.2 (d, J = 16 Hz, Ar), 140.8 (d, J = 19 Hz, =CHPh), 137.4 (d, J = 45 Hz, P–CH=), 136.9 (s, Ar), 129.6 (d, J = 10 Hz, CH Ar), 128.2 (s, CH Ar), 127.9 (s, CH Ar), 127.8 (s, CH Ar), 127.6 (d, J = 25 Hz, CH Ar), 127.3 (d, J = 8 Hz, CH Ar), 126.9 (s, CH Ar), 124.4 (s, CH Ar), 123.5 (s, CH Ar), 122.5 (s, CH Ar), 63.0 (d, J = 9 Hz, CH_2), 28.4 (s, CH), 28.3 (d, J = 5 Hz, CH), 25.1 (s, CH_3), 24.9 (s, CH_3), 24.8 (s, CH_3), 24.6 (d, J = 4 Hz, CH_3). ^1H and ^{13}C NMR assignments were supported by HSQC and DEPT experiments.

CRediT authorship contribution statement

Miranda P. Howard: Writing – original draft, Validation, Methodology, Investigation, Formal analysis, Conceptualization. **Preston M. Miura-Akagi:** Methodology, Investigation. **Timothy W. Chapp:** Visualization, Software, Methodology, Formal analysis. **Yuri J.H. Ah-Tye:** Visualization, Methodology, Investigation. **Tomoko Kitano:** Methodology, Investigation. **Daniel Y. Zhou:** Methodology, Investigation. **Landon G. Balkwill:** Formal analysis, Data curation. **Wesley Y. Yoshida:** Formal analysis, Data curation. **Amy L. Fuller:** Formal analysis, Data curation. **Glenn P.A. Yap:** Visualization, Validation, Software, Formal analysis, Data curation. **Arnold L. Rheingold:** Investigation, Formal analysis. **Gabriela L. Borosky:** Writing – original draft, Visualization, Validation, Software, Methodology, Investigation, Formal analysis, Data curation. **Kenneth K. Laali:** Writing – original draft, Visualization, Validation, Supervision, Project administration, Methodology, Investigation, Formal analysis, Data curation, Conceptualization.

Declaration of competing interest

The authors declare that they have no known competing financial interests or personal relationships that could have appeared to influence the work reported in this paper.

Data availability

Data will be made available on request.

Acknowledgments

A research visit by KKL to the MFC Laboratory facilitated this project. MFC thanks the University of Hawai'i at Mānoa (UHM) for laboratory space and in-house maintenance. MFC also thanks the National Science Foundation (NSF) for a CAREER Award (CHE-1847711) and the American Chemical Society Petroleum Research Fund (ACS-PRF: 65352-ND3) for support. Mass spectroscopic data was obtained at UHM on an Agilent 6545 Accurate-Mass QTOF-LCMS (NSF CHE-1532310). GLB

acknowledges financial support from Consejo Nacional de Investigaciones Científicas y Técnicas (CONICET). Access to computational resources from CCAD-UNC and CCT-Rosario Computational Center, members of SNCAD-MinCyT, Argentina, is gratefully acknowledged. TWC acknowledges support from Allegheny College. Elemental analyses were conducted by William Brennessel (University of Rochester).

Appendix A. Supplementary data

NMR Methods and Simulations. NMR spectra were acquired on Agilent 300 DD2 and Agilent 600 DD2 NMR spectrometers with VNMRJ4.2 software. The spectra were processed using MestReNova 14.3.0 and 14.2.1. **DFT Calculations.** Full details on the computational methods, additional figures of the optimized structures, and Cartesian coordinates of the optimized stationary points [31]. **X-ray crystallography.** All structures were obtained using Bruker rotating-anode diffractometers with Mo-K(alpha) radiation sources at 100K. Standard procedures using Bruker Apex software were used in all cases. Refinement programs were included in OLEX 2 software [32]. Details of the experiments are contained in the SI files. **Appendix A. Supplementary data.** CCDC contains the supplementary crystallographic data for structures 2300389, 2300390, and 2300391. These data can be obtained free of charge via http://www.ccdc.cam.ac.uk/conts/retrieving.html, or from the Cambridge Crystallographic Data Centre, 12 Union Road, Cambridge CB2 1EZ, UK; fax: (+44) 1223-336-033; or e-mail: deposit@ccdc.cam.ac.uk. Supplementary data to this article can be found online at https://doi.org/10.1016/j.poly.2024.116905.

References

[1] L.D. Quin, A Guide to Organophosphorus Chemistry, Wiley-Interscience, New York, 2000.
[2] (a) F. Mathey, The organic chemistry of phospholes, Chem. Rev. 88 (1988) 429–453;
(b) G. Fritz, P. Scheer, Silylphosphanes: developments in phosphorus chemistry, Chem. Rev. 100 (2000) 3341–3401;
(c) M.V. Jimenez, J.J. Perez-Torrente, I. Bartolome, L.A. Oro, Covenient methods for the synthesis of a library of hemilabile phosphines, Synthesis 11 (2009) 1916–1922.
[3] D. Gudat, A. Haghverdi, M. Nieger, Umpolung of P-H bonds, Angew. Chem. Int. Ed. 39 (2000) 3084–3086.
[4] D. Gudat, Diazaphospholenes: *N*-heterocyclic phosphines between molecules and Lewis pairs, Acc. Chem. Res. 43 (2010) 1307–1316.
[5] (a) M.R. Adams, C.-H. Tien, B.S.N. Huchenski, M.J. Ferguson, A.W.H. Speed, Diazaphospholene precatalysts for imine and conjugate reductions, Angew. Chem. Int. Ed. 56 (2017) 6268–6271;
(b) C.C. Chong, H. Hirao, R. Kinjo, Metal-free σ-bond metathesis in 1,3,2-diazaphospholene-catalyzed hydroboration of carbonyl compounds, Angew. Chem. Int. Ed. 54 (2015) 190–194;
(c) C.C. Chong, R. Kinjo, Catalytic hydroboration of carbonyl derivatives, imines, and carbon dioxide, ACS Catal. 5 (2015) 3238–3259.
[6] V. Kremlacek, J. Hyvl, W.Y. Yoshida, A. Ruzicka, A.L. Rheingold, J. Turek, R. P. Hughes, L. Dostal, M.F. Cain, Heterocycles derived from generating monovalent pnictogens within NCN pincers and bidentate NC chelates: hypervalency versus bell-clappers versus static aromatics, Organometallics 37 (2018) 2481–2490.
[7] D.Y. Zhou, P.M. Miura-Akagi, S.M. McCarty, C.H. Guiles, T.J. O'Donnell, W. Y. Yoshida, C.E. Krause, A.L. Rheingold, R.P. Hughes, M.F. Cain, P-alkynyl functionalized benzazaphospholes as transmetalating agents, Dalton Trans. 50 (2021) 599–611.
[8] P.M. Miura-Akagi, T.W. Chapp, W.Y. Yoshida, G.P.A. Yap, A.L. Rheingold, R. P. Hughes, M.F. Cain, Synthesis and structure of P-halogenated benzazaphospholes and their reactivity toward Pt(0) sources, Organometallics 42 (2023) 672–688.
[9] S. Burck, D. Gudat, K. Nattinen, M. Nieger, M. Niemeyer, D. Schmid, 2-Chloro-1,3,2-diazaphospholenes – a crystal structural study, Eur. J. Inorg. Chem. 5112–5119 (2007).
[10] A.W.H. Speed, Applications of diazaphospholene hydrides in chemical catalysis, Chem. Soc. Rev. 49 (2020) 8335–8353.
[11] J. Zhang, Y.-D. Yang, J.-P. Cheng, A nucleophilicity scale for the reactivity of diazaphospholenium hydrides: structural insights and synthetic applications, Angew. Chem. Int. Ed. 58 (2019) 5983–5987.
[12] S. Burck, D. Gudat, M. Nieger, W.-W. Du Mont, *P*-hydrogen-substituted 1,3,2-diazaphospholenes: molecular hydrides, J. Am. Chem. Soc. 128 (2006) 3946–3955.
[13] D.S. Glueck, Applications of 31P NMR spectroscopy in development of M(DuPhos)-catalyzed asymmetric synthesis of P-stereogenic phosphines (M = Pt or Pd), Coord. Chem. Rev. 252 (2008) 2171–2179.
[14] (a) M.K. Denk, S. Gupta, R. Ramachandran, Aromatic phosphenium cations, Tetrahedron Lett. 37 (1996) 9025–9028;
(b) C.J. Carmalt, V. Lomeli, B.G. McBurnett, A.H. Cowley, Cyclic phosphenium and arsenium cations with 6π electrons and related system, Chem. Commun. 2095–2096 (1997).
[15] A.H. Cowley, R.A. Kemp, Synthesis and reaction chemistry of stable two-coordinate phosphorus cations (phosphenium ions), Chem. Rev. 85 (1985) 367–382.
[16] R. Waterman, σ-Bond metathesis: A 30-year retrospective, Organometallics 32 (2013) 7249–7263.
[17] R.L. Melen, Dehydrocoupling routes to element-element bonds catalysed by Main group compounds, Chem. Soc. Rev. 45 (2016) 775–788.
[18] C. Ni, J. Hu, Recent advances in the synthetic application of difluorocarbene, Synthesis 46 (2014) 842–863.
[19] J.-H. Lin, J.-C. Xiao, Fluorinated ylides/carbenes and related intermediates from phosphonium/sulfonium salts, Acc. Chem. Res. 53 (2020) 1498–1510.
[20] Indazoles with $-CF_2H$ groups have related ^{19}F NMR spectra: D. Garcia-Perez, C. Lopez, R.M. Claramunt, I. Alkorta, J. Elguero, ^{19}F-NMR diastereotopic signals in two *N*-CHF_2 derivatives of (4S,7R)-7,8,8-Trimethyl-4,5,6,7-tetrahydro-4,7-methano-2H-indazole Molecules 22 (2017) 2003–2014.
[21] Examples of carbene insertion into P(V)–H derivatives are known: X. Mo, Y. Xie, L. Wei, X. Gu, M. Zhang, X. Zhang, J. Jiang, Visible-light-Induced carbene insertion into P–H bonds between acylsilanes and *H*-Phosphorus Oxides Org. Lett. 25 (2023) 2338–2343.
[22] S. Lau, T.M. Hood, R.L. Webster, Broken promises? On the continued challenges faced in catalytic hydrophosphination, ACS. Catal. 12 (2022) 10939–10949.
[23] D. Mimeau, A.-C. Gaumont, Regio- and stereoselective hydrophosphination reactions of alkynes with phosphine-boranes: access to stereodefined vinylphosphine derivatives, J. Org. Chem. 68 (2003) 7016–7022.
[24] L. Rosenberg, Mechanisms of metal-catalyzed hydrophosphination of alkenes and alkynes, ACS Catal. 3 (2013) 2845–2855.
[25] L. Routaboul, F. Toulgoat, J. Gatignol, J.-F. Lohier, B. Norah, O. Delacroix, C. Alayrac, M. Taillefer, A.-C. Gaumont, Iron-salt-promoted highly regioselective α and β hydrophosphination of alkenyl arenes, Chem. Eur. J. 19 (2013) 8760–8764.
[26] (a) J. Simon, U. Bergstrasser, M. Regitz, K. Laali, Synthesis of a doubly complexed bisphosphirenyl ether and generation of phosphirenylium cations complexed with pentacarbonyltungsten, Organometallics 18 (1999) 817–819;
(b) A. Jayaraman, B.T. Sterenberg, Electrophilic aromatic substitution reactions of a tungsten-coordinated phosphirenyl triflate, Organometallics 33 (2014) 522–530.
[27] Y. Moglie, M.J. Gonzalez-Soria, I. Martin-Garcia, G. Radivoy, F. Alonso, Catalyst- and solvent-free hydrophosphination and multicomponent hydrothiophosphination of alkenes and alkynes, Green Chem. 18 (2016) 4896–4907.
[28] R.G. Pearson, Hard and soft acids and bases, HSAB, Part 1, J. Chem. Educ. 45 (1968) 581–587.
[29] Miura-Akagi, P.M.; Cain, M.F. Unpublished results.
[30] (a) J.F. Buergler, A. Togni, Chiral trifluoromethylphosphines: A new stereoselective synthesis of *Josiphos*-type ligands containing two stereogenic phosphorus atoms, Chem. Commun. 47 (2011) 1896–1898;
(b) O. Shyshkov, U. Dieckbreder, T. Drews, A. Kolomeitsev, G.-V. Roschenthaler, K. Seppelt, The tris(trifluoromethyl)methyl phosphonium ion, $P(CF_3)_3CH_3^+$, Preparation and structure, Inorg. Chem. 48 (2009) 6083–6085.
[31] (a) M.J. Frisch, G.W. Trucks, H.B. Schlegel, G.E. Scuseria, M.A. Robb, J. R. Cheeseman, G. Scalmani, V. Barone, G.A. Petersson, H. Nakatsuji, X. Li, M. Caricato, A.V. Marenich, J. Bloino, B.G. Janesko, R. Gomperts, B. Mennucci, H. P. Hratchian, J.V. Ortiz, A.F. Izmaylov, J.L. Sonnenberg, D. Williams-Young, F. Ding, F. Lipparini, F. Egidi, J. Goings, B. Peng, A. Petrone, T. Henderson, D. Ranasinghe, V.G. Zakrzewski, J. Gao, N. Rega, G. Zheng, W. Liang, M. Hada, M. Ehara, K. Toyota, R. Fukuda, J. Hasegawa, M. Ishida, T. Nakajima, Y. Honda, O. Kitao, H. Nakai, T. Vreven, K. Throssell, J.A. Montgomery Jr., J.E. Peralta, F. Ogliaro, M.J. Bearpark, J.J. Heyd, E.N. Brothers, K.N. Kudin, V.N. Staroverov, T. A. Keith, R. Kobayashi, J. Normand, K. Raghavachari, A.P. Rendell, J.C. Burant, S. S. Iyengar, J. Tomasi, M. Cossi, J.M. Millam, M. Klene, C. Adamo, R. Cammi, J. W. Ochterski, R.L. Martin, K. Morokuma, O. Farkas, J.B. Foresman, D.J. Fox, Gaussian 16, Revision C.01, Gaussian Inc, Wallingford, CT, 2016;
(b) A.D. Becke, Density-functional thermochemistry. III. The role of exact exchange, J. Chem. Phys. 98 (1993) 5648–5652;
(c) C. Lee, W. Yang, R.G. Parr, Development of the Colle-Salvetti correlation-energy formula into a functional of the electron density, Phys. Rev. B: Condens. Matter Mater. Phys. 37 (1988) 785–789;
(d) S. Grimme, J. Antony, S. Ehrlich, H.J. Krieg, A consistent and accurate ab initio parametrization of density functional dispersion correction (DFT-D) for the 94 elements H-Pu, Chem. Phys. 132 (2010) 154104;
(e) K. Fukui, The path of chemical reactions - the IRC approach, Acc. Chem. Res. 14 (1981) 363–368;
(f) H.P. Hratchian, H.B. Schlegel, Finding minima, transition states, and following reaction pathways on ab initio potential energy surfaces, in: C.E. Dykstra, G. Frenking, K.S. Kim, G. Scuseria (Eds.), Theory and Applications of Computational Chemistry: The First 40 Years, Elsevier, Amsterdam, 2005, pp. 195–249;
(g) J. Tomasi, B. Mennucci, E. Cancès, The IEF version of the PCM solvation method: An overview of a new method addressed to study molecular solutes at the QM ab initio level, J. Mol. Struct. 464 (1999) 211–226;
(h) E.D. Glendening, A.E. Reed, J.E. Carpenter, F. Weinhold, NBO (Version 3.1), Gaussian Inc., Wallingford, CT, 2009.
[32] (a) O.V. Dolomanov, L.J. Bourhis, R.J. Gildea, J.A.K. Howard, H. Puschmann, OLEX2: a complete structure solution, refinement and analysis program, J. Appl. Cryst. 42 (2009) 339–341;
(b) L.J. Bourhis, O.V. Dolomanov, R.J. Gildea, J.A.K. Howard, H. Puschmann, The

anatomy of a comprehensive constrained, restrained refinement program for the modern computing environment – Olex2 dissected, Acta Cryst. A71 (2015) 59–75; (c) G.M. Sheldrick, A short history of SHELX, Acta Cryst. A64 (2008) 112–122.